NRL Report 7172

Aging of Barium Titanate and Lead Zirconate-Titanate Ferroelectric Ceramics

JULES DELAUNAY AND PAUL L. SMITH

Crystal Physics Branch
Solid State Division

October 15, 1970

NAVAL RESEARCH LABORATORY
Washington, D.C.

CONTENTS

ABSTRACT

The report reviews the present knowledge of the aging process in barium titanate and lead zirconate-titanate ferroelectric ceramics. By "aging" is meant the passive change in the mechanical and electrical properties of a ferroelectric with time. Experimental data show that these constants vary linearly with the logarithm of time. The Smith, Street and Woolley, and Plessner theories for this logarithmic dependence are revised to remove some of the obscurity in the usual derivation. The experimental evidence of Ikegami and Ueda and of Bradt and Ansell, which is described in some detail, supports the hypothesis that aging is associated with the relief of internal stress through the formation of 90°-domains.

The properties of lead zirconate-titanate can be changed to some extent by chemical additives. Such additions may also change the aging rate. In particular, it has been found that trivalent and pentavalent ions substituted for bivalent lead decrease the rate by a factor of 5 to 10. On the other hand, additives which cause an oxygen deficiency (e.g., Fe) have little effect on the aging rate. A class of chemicals (e.g., Cr) called "thermally variable ions" by Jaffe, because of the apparent temperature dependence of their valence, holds promise for lowering the aging rate without adversely affecting the high-drive sonar transducer characteristics of the material.

Suggestions are made for further research.

PROBLEM STATUS

This is an interim report reviewing the present state of knowledge of the aging process.

AUTHORIZATION

NRL Problem P03-03
Project SF 11-121-303/14082

Manuscript submitted July 31, 1970.

AGING OF BARIUM TITANATE AND LEAD ZIRCONATE-TITANATE FERROELECTRIC CERAMICS

INTRODUCTION

The ferroelectric materials used for sonar transducers are the perovskites: barium titanate ($BaTiO_3$) and lead zirconate-titanate. The second material is the solid solution $(PbZrO_3)_x + (PbTiO_3)_{1-x}$ called PZT.* These perovskites suffer the disadvantage (among others) that their electrical and mechanical properties change as a function of time. Such a change is called "aging," referred to as "shelf-aging" at times to emphasize the passive nature of the change. It is observed in both poled and unpoled ceramics and in single crystals. The change is such that the dielectric constant K, the piezoelectric constant d, and the elastic compliance constants s all decrease linearly with the logarithm of the time. This report reviews the present knowledge of the aging process for $BaTiO_3$ and PZT and suggests ideas for further research.

BARIUM TITANATE

Background Information

Figure 1 shows the arrangement of the ions in a unit cell of $BaTiO_3$ when this compound is in its paraelectric state. In this state, which occurs above 120°C, $BaTiO_3$ has a cubic structure; it is nonferroelectric, nonpiezoelectric, and its electrical susceptibility obeys a Curie-Weiss law. The titanium ion is in the center of an octahedral cage of oxygen ions (see Fig. 2). As the temperature is lowered below 120°C, the Ti ions move spontaneously from the centers of the oxygen cages toward one or the other of the six oxygen neighbors. It is this displacement (when it happens cooperatively) which gives the dipole moment associated with ferroelectricity.

The fact that the perovskites have cubic symmetry in the paraelectric state has made this class of materials seem relatively simple, and so they have received much theoretical and experimental attention, particularly $BaTiO_3$. On the other hand, the very fact that the dipole moment can occur equally well along any one of three mutually perpendicular directions is at the basis of some of the complicated behavior described in this report. If the Ti displacements occur in the same direction throughout a crystal, then the crystal consists of a single ferroelectric domain and the situation is rather simple. Usually, however, the domains nucleate independently at various places in the crystal while it is cooled through its transition temperature (120°C). The direction of the spontaneous moment of any of the nuclei may occur along any of the three principal cubic axes, depending on chance variations in composition and temperature. These nucleated domains grow until they encounter one another. A crystal at room temperature will thus be found to consist of a number of ferroelectric domains with polarization directions of some at right angles to those of others. Figure 3 is a schematic diagram of a collection of such domains. The common face of two domains polarized at 90° to one another is a "90°-wall." Figure 3 shows these walls as regions of "head-to-tail" confrontations for the avoidance of space charges. The common surface of two domains polarized at 180° to one another is a "180°-wall."

*"PZT" is the Clevite Corporation trade name of these ceramics. It is used in this report as a convenient abbreviation.

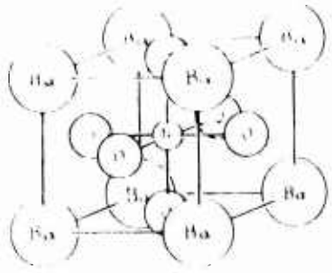

Fig. 1 - The ions of $BaTiO_3$ are arranged in the crystal as shown in this diagram of a unit cell. The titanium ion is in the center of the cube, the barium ions are at the corners, and the oxygen ions are at the face centers.

Fig. 2 - The same ion configuration as in Fig. 1, but with the Ba ions removed to reveal the Ti ion in the center of its octahedral oxygen cage

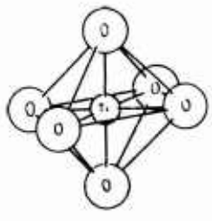

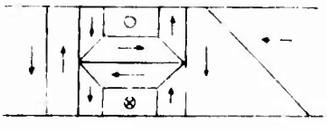

Fig. 3 - A (100) section through a multidomain $BaTiO_3$ crystal illustrating schematically an arrangement of the domains. The arrows are in the direction of the domain polarization.

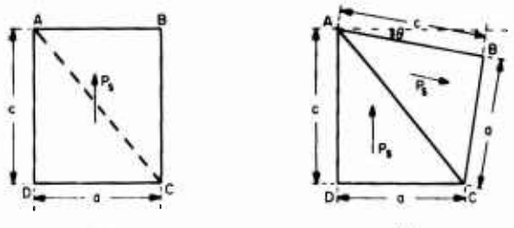

Fig. 4 - Parts (a) and (b) are drawn to the scale $c/a = 7/6$, which is an exaggeration. (a) Single domain crystal with spontaneous polarization P_s. (b) Two domains with the polarizations of the two making about 90° with one another. The departure of the angle (DAB) from 90° is labeled θ.

When the Ti ion shifts toward one of the oxygen neighbors, the unit cell loses its cubic symmetry and its shape changes from cubic to tetragonal. The principal axis parallel to the direction of this shift is elongated and becomes the tetragonal c axis. The other two axes contract and become the a axes. The deformation is not large, the c/a ratio for $BaTiO_3$ at room temperature being about 1.01. Nevertheless, this departure of the domains from cubic symmetry gives rise to internal stresses. Figure 4 illustrates how this comes about. Imagine a single crystal of $BaTiO_3$ in the form of a cube while it is in the paraelectric state, the cube surfaces being parallel to the (100) family of crystal planes. In the ferroelectric state, the cube assumes the shape shown in Fig. 4a if it consists of a single ferroelectric domain. Next, suppose that this domain becomes two domains, the second domain being polarized at 90° in the manner shown in Fig. 4b. The angle ω shown in Fig. 4b is approximately $(c - a)/a$. For $BaTiO_3$, $(c - a)/a \approx 0.01$ at room temperature so that ω is about 34 minutes of arc. Thus, even though the angle between the two directions of polarization is about 89° 26′, we shall continue to use expressions such as "90°-wall." It is clear that a large number of domains joined together by 90°-walls must be under internal stress, since the domains must be elastically deformed in order to fill the crystal continuously.

Aging of the Dielectric Constant

The first published account of the aging of ferroelectric ceramics is that of Marks (1) in 1948. Figure 5 shows the aging of the dielectric constant of two ceramic samples of $BaTiO_3$, each containing a chemical additive. Similar aging has been observed in the pure $BaTiO_3$ ceramic (2).

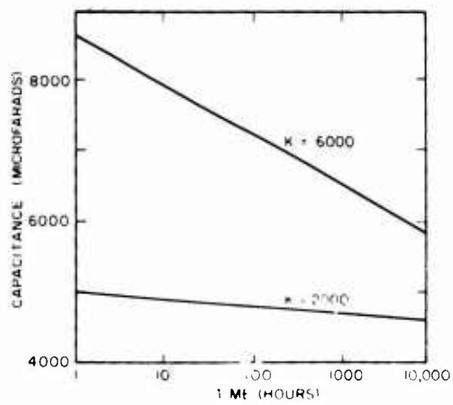

Fig. 5 - Aging curve of two samples of $BaTiO_3$ ceramic both containing added impurities

The main point of interest is that the decay in the dielectric constant is not exponential, but logarithmic. That is, the aging of the dielectric constant K does not obey the standard decay law

$$K(t) \quad K(0)e^{-\alpha t},$$

but rather

$$K(t) = K(1)(1 - \beta \log t). \qquad (1)$$

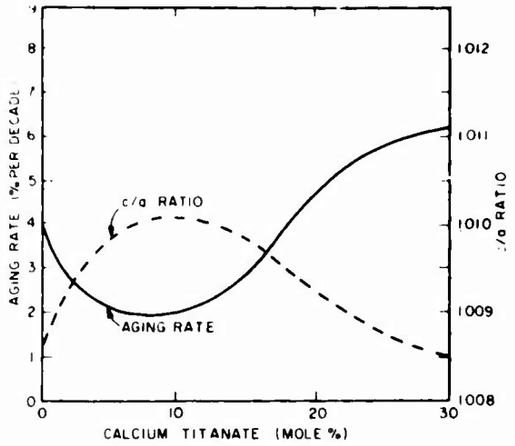

Fig. 6 - Effect of calcium titanate additions on the aging rate of barium titanate and variations of the c/a ratio of the unit cell with the mole percent of calcium titanate present

Here, t is the time, K(0) is the value of K at t = 0, and K(1) is its value at t = 1. The slopes of the straight lines were observed to remain constant for more than a year.

Marks also states that when these ceramics are raised to a temperature of 85°C or higher for a few minutes, then cooled back to room temperature, the dielectric constant returns to its original K value, and the aging starts anew. For pure $BaTiO_3$, 85°C would be below its transition temperature, which is about 120°C. The modified samples, however, appear to have transition temperatures just below 85°C. Thus, we have the empirical rule: If the sample is heated to above its transition temperature and held in the paraelectric state for several minutes, then cooled again to room temperature, the dielectric constant recovers its original value K(1) and the aging starts all over again.

The aging data are customarily plotted on semilog graph paper, which is equivalent to plotting the quantity Q(t) as

$$Q(t) = Q(1)(1 - c \log_{10} t). \tag{2}$$

The aging is then conveniently given as the value of c expressed in units of percent change in Q per decade of time. Thus, if we denote the aging rate in these units by c', we have

$$c' = 100c = 100 \frac{Q(t) - Q(10t)}{Q(1)}. \tag{3}$$

A further study of the aging of the dielectric constant of barium titanate ceramic was conducted in 1955 by McQuarrie and Buessem (2). They found the logarithmic dependence on time described by Marks. Heat treatment of the ceramic to temperatures below the transition temperature caused a partial recovery of the dielectric constant. If the heat treatment takes place above the transition temperature, full recovery occurs. They also examined the aging rate of barium titanate alloyed with calcium titanate. Figure 6 exhibits the aging rate as a function of composition for these materials. Included in the figure is a plot of the c/a ratio, which shows that the larger the c/a ratio the lower the aging rate.

This finding is consistent with another of their results, namely, that the aging rate increases as the temperature of the sample approaches the transition temperature from below. Since the c/a ratio of a given ceramic decreases as the temperature increases toward the transition temperature, the suggestion is that the aging rate is controlled at least in part by the degree of "tetragonality" of the specimen.

Theory of the Logarithmic Time Dependence of Aging

The difficulty in formulating a semiphenomenological theory of aging is in obtaining a logarithmic time dependence. For example, Mason's theory (3) leads to an aging law of the form $A/(1+Bt)$, which does not agree with experiment (4). Yet logarithmic decay is observed in a number of phenomena. Smith (5) developed a theory for transient creep in metals, and though his formula does not give a strictly logarithmic dependence, it manages to squeeze out such a dependence under certain conditions (see the derivation below). Magnetic viscosity is another phenomenon showing a logarithmic time dependence. The explanation of this phenomenon is that the magnetic domain walls are trapped in shallow energy wells and that the domain walls are lifted from their traps by thermal agitation. Street and Woolley (6) took the theory of Smith for creep in metals and adapted it to magnetic viscosity, mostly because they knew that it would lead to the observed logarithmic time dependence. Plessner (4) then took over the Street and Woolley form of the Smith theory in toto as the theory of aging of the dielectric constant of ferroelectrics. We shall sketch this theory here.

Plessner's view of domain wall motion is that these walls are in various kinds of energy traps (unspecified). Two neighboring shallow traps are shown at A and B in Fig. 7. An applied electric field can force a well to move from trap A to B, or from B to A. Now consider the neighboring wells at C and D. The well at C is shallow and has the activation energy E. In the course of time, thermal energy will cause the wall to move over the potential hump between C and D and drop into the deep well at D. Once in D, the domain wall cannot be moved by an electric field in the manner of those at A and B, or the one at C which could perhaps move to another shallow well, and so it becomes electrically inactive. It takes no part in the portion of the dielectric constant arising from domain wall motion.

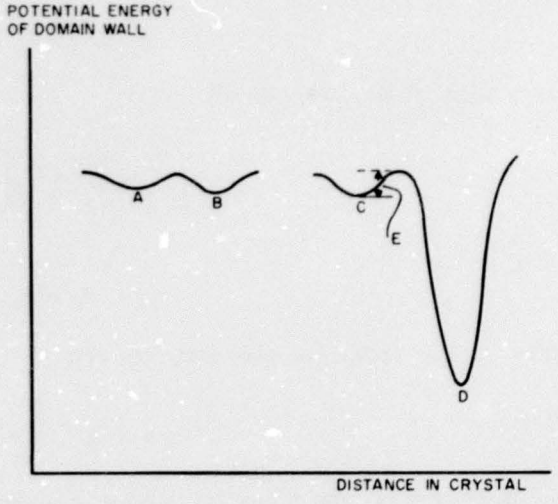

Fig. 7 - Potential well traps for domain walls

The problem before us is to calculate the value of N_D, the number of domain walls caught in deep traps such as at D, as a function of time, on the basis of this model. The source of activation of this process will be the thermal agitation represented by the Boltzmann factor $\exp(-E/kT)$. The reservoir of sites such as C and D is assumed to be limited in that the growth of N_D reflects a depletion of N_C.

Let there be N_C domain walls at traps such as C in Fig. 7 at some time t, and N_D in the deep well at D. At $t = 0$, we have $N_C = N_0$ and $N_D = 0$. At later times N_C has decreased from its initial value N_0 and N_D has increased. At all times, the relation between N_C and N_D will be

$$N_C + N_D = N_0 = \text{constant}. \tag{4}$$

Now let $\rho_D\, dE$ be the portion of N_D contained in the narrow energy range between E and $E + dE$. The time rate of change of ρ_D is proportional to the Boltzmann factor and to the number of domains available in states such as C; that is,

$$\frac{d\rho_D}{dt} = A\rho_C e^{-E/kT}. \tag{5}$$

Here, A is the constant of proportionality. The symbol ρ_C is defined similarly to ρ_D; that is, $\rho_C\, dE$ is the portion of N_C contained in the narrow energy range between E and dE. Defining a ρ_0 in a similar way to correspond to N_0 and making use of Eq. (4), we have that

$$\rho_C = \rho_0 - \rho_D, \tag{6}$$

so that,

$$\frac{d\rho_D}{dt} = A(\rho_0 - \rho_D) e^{-E/kT}. \tag{7}$$

We next introduce the symbol λ defined by

$$\lambda(E) = Ae^{-E/kT}. \tag{8}$$

Then, Eq. (7) becomes

$$\frac{d\rho_D}{dt} = \lambda(\rho_0 - \rho_D). \tag{9}$$

The integration of Eq. (9), namely

$$\int_0^{\rho_D} \frac{d\rho_D}{\rho_0 - \rho_D} = \int_0^t \lambda\, dt$$

gives

$$\rho_0 - \rho_D = \rho_0 e^{-\lambda t}. \tag{10}$$

Substitute $\rho_0 - \rho_D$ from Eq. (10) into Eq. (7):

$$d\rho_D = A\rho_0 e^{-\lambda t} e^{-E/kT}\, dt.$$

Now the number N_D of the domains moving into wells of type D for the whole spectrum of energies is given by

$$N_D = \int_0^{\infty} \rho_D \, dE,$$

or

$$N_D = A \int_0^t \int_0^{\lambda} \cdot_0 e^{-\cdot t} e^{-E/kT} \, dt \, dE. \tag{11}$$

We do not know what the initial spectrum $\cdot_0(E)$ is, so we follow Smith in putting ρ_0 = constant ("white" spectrum). Thus,

$$N_D = A \cdot_0 \int_0^t \int_0^{\infty} e^{-\cdot t} e^{-E/kT} \, dt \, dE. \tag{12}$$

The parameter $\cdot$ is a function of E (see Eq. (8)). The integration over E can be simplified by changing the variable of integration from E to λ. From Eq. (8), we have

$$\log \lambda = \log A - E/kT.$$

Differentiation of this expression gives

$$dE = -\frac{kT \, d\lambda}{\lambda}. \tag{13}$$

Consequently, we simplify the expression for N_D to

$$N_D = \rho_0 kT \int_0^t \int_0^{A} e^{-\lambda t} \, d\cdot \, dt$$

$$= \rho_0 kT \int_0^t \frac{1 - e^{-At}}{t} \, dt. \tag{14}$$

The integral which occurs in Eq. (14) has essentially a logarithmic dependence on t after a sufficiently long time has elapsed. This is revealed in the following analysis.

First the integral is simplified by putting $\tau = At$. Then it becomes the integral $I(\tau)$ defined by

$$I(\tau) = \int_0^{\tau} \frac{1 - e^{-\tau}}{\tau} \, d\tau. \tag{15}$$

The value $\tau = 1$ corresponds to $t = 1/A$ of the original integral.

Figure 8 shows, as the upper curve, a plot of the exact function $I(\tau)$ defined by Eq. (15). The lowest of the three curves is a plot of $\log \tau$. For $\tau > 2$, the two curves just mentioned become almost parallel. To find the vertical distance of separation C, we need to evaluate

$$\lim_{\tau \to \infty} [I(\tau) - \log \tau];$$

that is,

$$\lim_{\tau \to \infty} \left(\int_0^{\tau} \frac{1 - e^{-\tau}}{\tau} \, d\tau - \log \tau \right) = C. \tag{16}$$

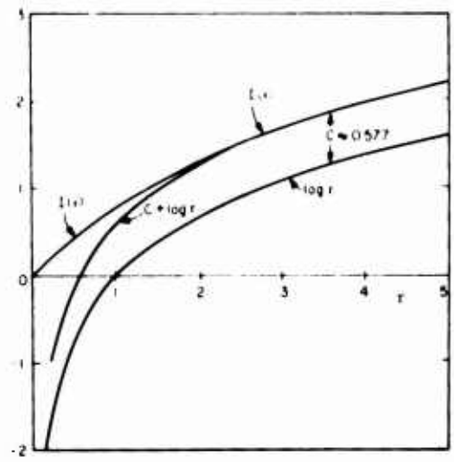

Fig. 8 - The uppermost curve is a plot of $I = \int_0^\tau \left[(1 - e^{-\tau})/\tau\right] d\tau$. The lowest curve is a plot of log τ (base e). The middle curve is the lowest curve displaced upward by an amount C (Euler's constant).

Now log τ can be expressed as

$$\log \tau = \int_1^\tau \frac{d\tau}{\tau} .$$

Hence, Eq. (16) can be conveniently reexpressed as

$$\lim_{\tau \to \infty} \left(\int_0^1 \frac{1 - e^{-\tau}}{\tau} d\tau + \int_1^\tau \frac{1 - e^{-\tau}}{\tau} d\tau - \int_1^\tau \frac{d\tau}{\tau} \right)$$

$$= \lim_{\tau \to \infty} \left(\int_0^1 \frac{1 - e^{-\tau}}{\tau} d\tau - \int_1^\tau \frac{e^{-\tau}}{\tau} d\tau \right).$$

Thus, we have that

$$C = \int_0^1 \frac{1 - e^{-\tau}}{\tau} d\tau - \int_1^\infty \frac{e^{-\tau}}{\tau} d\tau.$$

These integrals are easily evaluated numerically. The first is just the rapidly converging series

$$1 - \frac{1}{2 \cdot 2!} + \frac{1}{3 \cdot 3!} - \frac{1}{4 \cdot 4!} + \frac{1}{5 \cdot 5!} - \ldots = 0.796\ldots$$

obtained by expanding $\exp(-\tau)$ about $\tau = 0$ and integrating term by term. The second can be converted to an integral over the finite range $0 \leq x \leq 1$ by using the transformation $\tau = 1 \; x$. The trapezoidal rule gives its value to six significant figures with a division of the interval of integration into only 20 parts. The result is

$$C = 0.796599599 - 0.219383934 = 0.577215665.$$

We see that C is none other than Euler's constant.

We have arrived at the fact that the behavior of I becomes closely logarithmic at $\cdot \cdot 2$, i.e., at $t \cdot 1\,2A$. The middle curve of Fig. 8 shows the log τ curve displaced upward by Euler's constant and demonstrates clearly the point which we are making. Another fact which is revealed is that asymptotic approach of I is to C + log τ and not to just log τ.

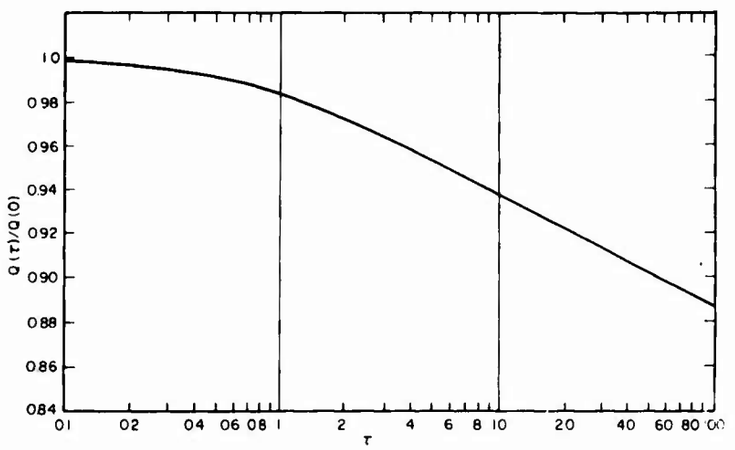

Fig. 9 - A plot of $Q(\tau)/Q(0)$ for 5% per decade aging rate, according to Eq. (18)

From this, we see that at time $t = 1/2A$, a good approximation to the value of N_D is

$$N_D \approx \rho_0 kT(C + \log \tau), \quad \tau > 2.$$

If we define a time t_0 by $t_0 = 1/A$, then τ becomes t/t_0 and we write the above approximation to N_D as

$$N_D \approx \rho_0 kT(C + \log \frac{t}{t_0}), \quad t > 2t_0.$$

The part of the dielectric constant attributable to domain wall motion should be proportional to N_C (besides N_A, N_B), i.e., to those walls not trapped by deep wells. Thus, the dielectric constant K is

$$K \propto N_C = N_0 - N_D,$$

which states that the time dependence of K is of the form

$$K(t) = K(t_0)(1 - \alpha \log \frac{t}{t_0}). \tag{17}$$

This is the result we set out to demonstrate, and corresponds to Eq. (1).

Finally, it is interesting to see a plot on semilog paper of the aging of a quantity $Q(\tau)$ according to the exact function $I(\tau)$. For this purpose, we shall adopt an aging rate of 5% per decade. This amounts to $5 \times \log 10$ or 2.17% per factor e of time. Therefore, we plot the relation

$$Q(\tau) = Q(0) = 1 - 0.0217 \int_0^{\tau} \frac{1 - e^{-\tau'}}{\tau'} d\tau'. \tag{18}$$

Notice that it is more convenient to use the normalizing constant $Q(0)$ here instead of $Q(1)$. Figure 9 shows the graph of Eq. (18). At $\tau = 0.1$, Q is about $0.995\,Q(0)$. Beyond $\tau = 2$, the curve is practically a straight line.

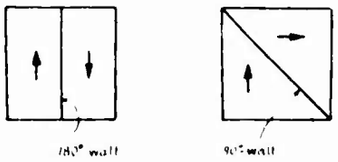

Fig. 10 - Illustration of a 180°-wall (left) and a 90°-wall (right)

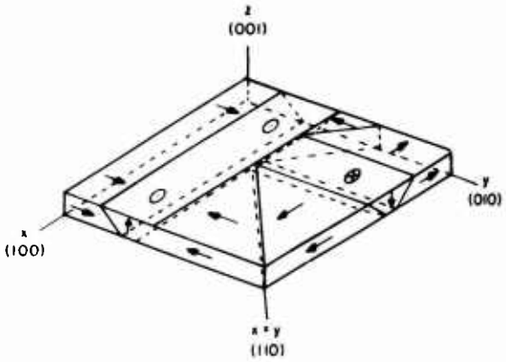

Fig. 11 - Illustration of a variety of domains and their walls

Formation of 90°-Domains During Aging

Thus far, we have seen that aging has been ascribed to the gradual relaxation of the domain configurations to ones of greater stability, thereby reducing some of the internal stresses arising from the tetragonality of the domains. This occurs in both single crystals and polycrystalline samples, and both in poled and unpoled samples. In order to discover the nature of these domain readjustments, Ikegami and Ueda (7) and Bradt and Ansell (8,9) have made direct observations of the domain structures in $BaTiO_3$ as a function of the time after cooling the samples through the transition temperature. We shall first explain the terms commonly used in the discussion of such investigations. Then we shall give a summary of the results and conclusions published by the above mentioned authors.

The domain patterns observed on crystal surfaces are delineated by domain walls and so the emphasis is on the walls rather than on the domains themselves. Two kinds of walls are identified in multidomain structures in the tetragonal phase of the ferroelectric perovskites, and they are illustrated in Fig. 10. One is the wall between two domains of parallel but oppositely directed polarizations and is therefore called a "180°-wall." Such a wall is parallel to a (100)-type crystal plane (i.e., to (100), (010), (001) planes). Observations indicate that its thickness is either about one unit cell (4 Å) or perhaps zero. In the former case, the 180°-wall would consist of a single layer of unit cells having zero polarization. In the second case, the wall would simply be a mathematical plane across which the polarization abruptly reverses.

The other type of domain wall is the "90°-wall," which separates two neighboring domains with polarization directions at right angles to one another. The illustrative sketch in the right half of Fig. 10 is a simplified version of Fig. 4b and neglects the elastic distortion associated with such configurations. The polarizations in the figure have been chosen in the "head-to-tail" confrontation, rather than "head-to-head," in order that there be no charge on the wall. Experimental observations give the thickness of this wall to be somewhere between 60 Å and 100 Å (e.g., consult Ref. 9).

Figure 11 shows a crystal plate consisting of a miscellaneous collection of domains. The edges are along the principal directions (fourfold axes of the original paraelectric crystal of cubic symmetry). In Figs. 12, 13, 15, and 16 to follow, this same aspect is maintained. The nomenclature introduced below is based on the line of sight of the experimenter. His eye is above the plate and he is looking downward at it along the z axis. Now a domain with its polarization parallel to the line of sight (parallel to z or (001)) has the

c axis of its unit cells along this direction and is called a "c-domain." The other domains have their c axis in the x,y plane and thus are viewed along one of their two a axes. Such domains are therefore called "a-domains." There is no physical difference between a c-domain and an a-domain, except that at the surface there is greater opportunity for elastic yield to internal stresses than in the bulk of the sample and this will make some difference at the surface. However, the nomenclature is not devised to take this into account but solely to describe the observations at the surfaces of plates, of single crystals, and of single crystallites in polycrystalline samples (i.e., ceramics).

In Fig. 11, two c-domains are shown: the one with the dot-centered circles is polarized upward and the other with the cross-centered circles is polarized downward. The remaining domains are a-domains. The arrows show the direction of polarization. There are two kinds of 90°-walls, and they are both shown in the figure. A wall between two a-domains is an "a-a wall" and is always a plane of the (110) type (i. e., parallel to an $x = \pm y$ plane). A wall between a c-domain and an a-domain is a "c-a wall." It is always parallel to a plane of the (011) type (i.e., parallel to one of the planes $z = \pm x$, $z = \pm y$). The trace of a c-a wall on the surface is a straight line (in the ideal case) parallel to the x or y axes. Thus, on the surface, c-a and a-a walls are distinguishable by the fact that the former are along (100)-type directions and the latter make 45° to these directions.

Between two oppositely oriented c-domains, there should exist a 180°-wall. Figure 11 does not show this wall, but rather a continuation of the c-a wall. This means that in the diagram the c-a wall between the two c-domains is a tail-to-tail confrontation. If this segment of the c-a wall is replaced by a proper c-c wall, then the junction of this c-c wall with the c-a and a-a walls no longer match up electrically. An effort to design a proper electrically neutral set of walls results in considerable local elastic deformation at the intersection. We thus expect such a corner to be a region of high internal stress in the real crystal.

The observed domain patterns often appear as sets of parallel domain walls. Figures 12 through 16 show a number of domain wall patterns constructed using the head-to-tail confrontation principle. Figure 12 shows two patterns composed of a-a walls. A pattern congruent to the lower one in the figure can be made with parallel a-a walls running perpendicular to the direction of the Fig. 12 sketch. Either pattern can occur in the crystal. When two such patterns meet, they do so along a (100)-type plane as shown in Fig. 13. An assembly of such sets can result in the "herring-bone" pattern shown in Fig. 14. Figure 15 shows another pattern consisting of a set of parallel walls, but the traces of these walls in the upper surface are now parallel to a principal axis (x or y) because they are traces of c-a walls. Two sets of such patterns are possible and Fig. 16 shows a pair meeting along a plane of the (110) type. An extended assembly of such sets can also lead to herring-bone patterns but rotated at 45° to the type of herring-bone pattern mentioned earlier.

Finally, there is another pattern frequently observed and that is a set of parallel domain walls encountering another set of parallel domain walls, the angle between the two sets of parallel lines being 45° (or 135°). This can occur when a set of a-a domains (lower half of Fig. 12) abuts on a set of c-a domains (Fig. 15). As mentioned toward the end of the discussion of Fig. 11, the junction of the two sets should be a region of high internal stress.

Ikegami and Ueda (7) worked with polycrystalline $BaTiO_3$, making their observations with both optical and electron microscopes. The samples were highly polished plates which were etched to reveal the domains. The etched surfaces were observed under a polarizing microscope at a magnification of 8.5* and with an electron microscope at a magnification of 2500 using a two-step replica technique. The observations were made at 10 minutes, 100 minutes, and 1000 minutes after the samples were cooled through the transition

*This is a rather low magnification. Perhaps it is a misprint.

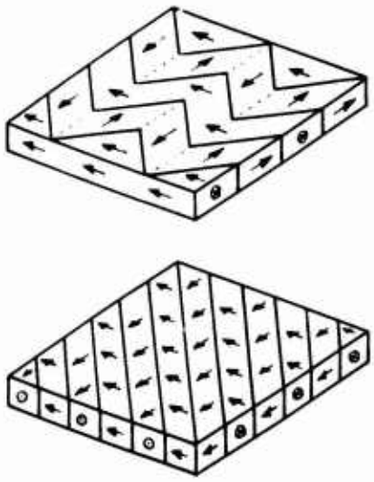

Fig. 12 - Two patterns constructed from a-a 90°-domain walls. The direction of the crystal axes is the same as in Fig. 11.

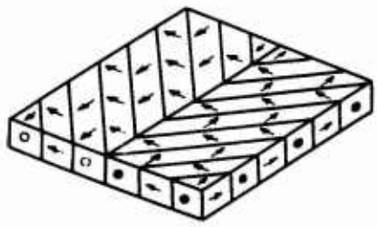

Fig. 13 - Two sets of a-a 90°-domain wall patterns of the type shown in the lower sketch of Fig. 12 meeting in a plane of the (100) type

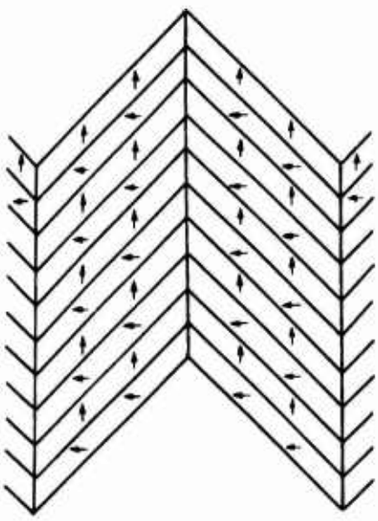

Fig. 14 - Extension of the pattern shown in Fig. 13, leading to a herring-bone pattern

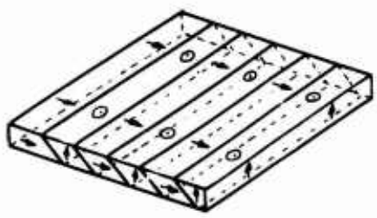

Fig. 15 - A pattern formed of parallel c-a 90°-domain walls

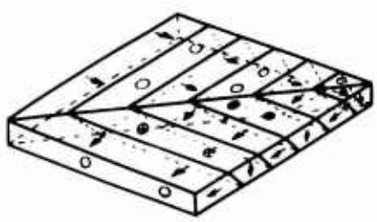

Fig. 16 - Two sets of c-a 90°-domain walls, such as the set shown in Fig. 15, meeting at a (110)-type plane

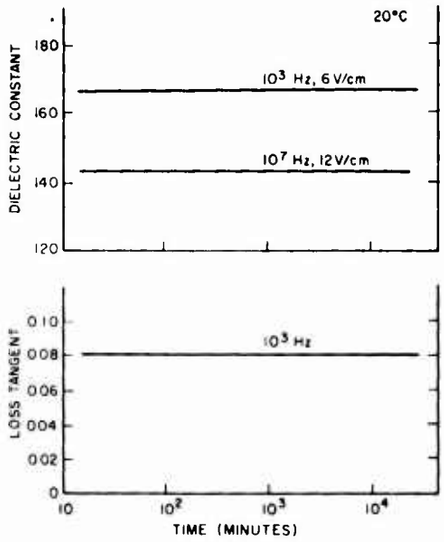

Fig. 17 - Aging of dielectric constant and loss tangent of polycrystalline $PbTiO_3$ containing 1-mole-percent MnO_2

temperature. At the 10-minute observation, no domain patterns were discernible. At the 100- and 1000-minute observations, sets of fine parallel "stripes" (about equally spaced) appeared. According to their published photographs (2500 magnification), the surface of a grain may contain only one set of parallel stripes (or lines). This set could consist of a-a walls or of c-a walls because the principal axes of none of the crystallites were identified. However, the main point is that these are 90°-wall patterns. One grain clearly shows two sets of parallel lines making 45° (or 135°) to one another, indicating the presence of both a-a and c-a domain walls. Ikegami and Ueda's explanation of aging is therefore the splitting up of larger domains into smaller domains with 90°-walls during the passage of time. They refer to this explanation as the "90°-splitting model," in contrast to the 180°-splitting model of Stankowski (10) whom they cite. They view the aging of the dielectric constant of $BaTiO_3$ ceramic as an increase in the clamping of the domains with increase in 90°-domain splitting with the passage of time. (This clamping is consistent with the entrapment of domain walls in deep D traps as in Fig. 7.)

Ikegami and Ueda consider that the remarks of McQuarrie and Buessem (2) on the relation of aging to degree of tetragonality (see Fig. 6 and its accompanying text) to be compatible with the 90°-splitting model. The McQuarrie-Buessem data were for barium titanate containing some calcium titanate, and the range of tetragonality available was $1.0085 \leq c/a \leq 1.011$. Now $PbTiO_3$ has the rather large c/a ratio of 1.06. For this reason, Ikegami and Ueda measured the aging of the dielectric constant and loss tangent of a polycrystalline sample of this material and, as they no doubt anticipated, found the aging to be too small to observe (see Fig. 17).

Further advances on 90°-domain formation as an aging phenomenon were made by Bradt and Ansell (8,9). Their observations were made primarily on thin single-crystal plates of $BaTiO_3$ grown by a modified Remeika technique. These plates have the aspect of Fig. 11 except that the section in the x,y plane is triangular instead of square. Domain patterns were observed both with a polarizing microscope (magnifications 50 to 250) and by means of a transmission electron microscope technique (magnifications to 70,000). The latter technique has the advantage over the replica technique in that it does not require chemical etching for the disclosure of the domain patterns.

Whenever the crystal was viewed in the polarizing microscope while it was being cooled through the transition temperature (120°C), the ferroelectric region would be seen sweeping across the crystal with a well-defined front. The ferroelectric region always began in the same place but different domain patterns appeared each time. As the samples aged, various sets of parallel a-a or c-a walls developed. The c-a walls predominated. The predominance is probably peculiar to thin plates, since c-a walls are tilted at 45° with respect to the upper and lower free surfaces, in contrast with a-a walls, and so their formation can be accompanied by a greater relief of stress at the free surface.

Bradt and Ansell could actually observe 90°-domains nucleate and made the important discovery that the nucleation takes place in or near regions where c-a and a-a domains occur together. This is probably because the juncture of these two types of domains is a region of high stress, as we have already mentioned. Furthermore, they found that the growth of the new domains was smooth, not jerky or jagged as one would expect if the growth involved defect structures. Sets (or "colonies") of domain walls move as a unit and are stopped suddenly as a unit when encountering another set or some invisible barrier.

Another interesting item in their papers concerns the contrast in the aging properties of single crystals and polycrystalline samples (ceramics). First, the dielectric constant of their ceramic material was considerably larger than that of the Remeika-type crystals, 4000 as compared to 1500. Second, the aging rate of the ceramic samples was larger than that of the single crystals by a factor of about two. Third, the aging rate of the ceramic samples was more reproducible from one aging run to another than for a single crystal. The higher dielectric constant is explained by the authors on the basis of higher internal stress in polycrystalline samples: the stress increases the dielectric constant. The superior reproducibility of the aging rate was attributed to the much higher density of 90°-domains present in the ceramic. This suggests that the origin of the better reproducibility is statistical rather than physical.

LEAD ZIRCONATE-TITANATE (PZT)

Background Information

At 490°C, pure $PbTiO_3$ undergoes a phase transition from a paraelectric state of cubic symmetry above this temperature to a ferroelectric state of tetragonal symmetry below it. $PbZrO_3$ is also a paraelectric substance above its transition temperature (230°C) but undergoes a phase change at this temperature to an antiferroelectric state of orthorhombic symmetry. Both substances have unit cells analogous to that of $BaTiO_3$, with Pb replacing Ba. Figure 18 illustrates their structures.

Solid solutions of $PbZrO_3$ and $PbTiO_3$ can be prepared in any proportion, yielding a graduation of physical properties, at room temperature, all the way from those of antiferroelectric $PbZrO_3$ to those of strongly ferroelectric $PbTiO_3$. Figure 19 shows a phase diagram of the PZT solid solution system, as worked out by Sawaguchi (11). The boundary near the 50-50 composition, separating the tetragonal from the trigonal ferroelectric phases, is called the "morphotropic" boundary.

We have already mentioned that the c/a ratio for pure $PbTiO_3$ is rather large (1.06) compared to that of $BaTiO_3$ (see Fig. 17 and the discussion of it in the accompanying text). Figure 20 gives the value of c and a of a unit cell of PZT as a function of the concentration of $PbTiO_3$, according to Shirane, Suzuki, and Takeda (12). It should be noticed that c/a is greater than unity for the ferroelectric phases and less than unity for the antiferroelectric phase.

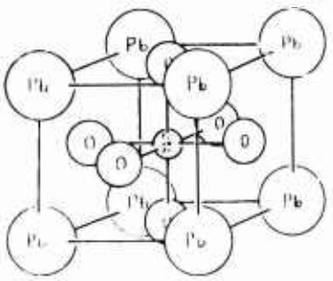

Fig. 18 - The unit cell of $PbTiO_3$ or $PbZrO_3$, depending on whether the central ion is Ti or Zr. In PZT, both cells are present, some with Ti ions and some with Zr ions at the central position.

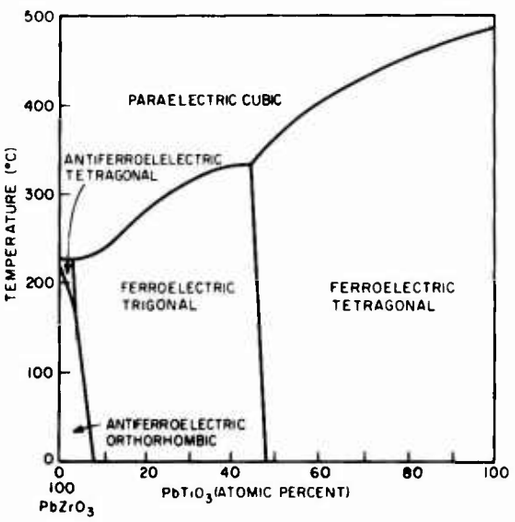

Fig. 19 - Phase diagram of the $PbZrO_3$-$PbTiO_3$ system

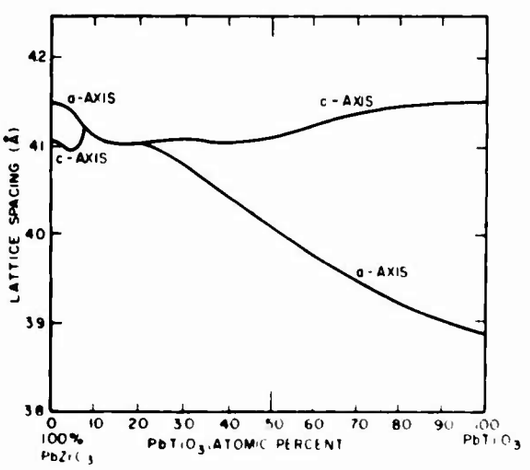

Fig. 20 - Lattice spacing of the $PbZrO_3$-$PbTiO_3$ solid solutions

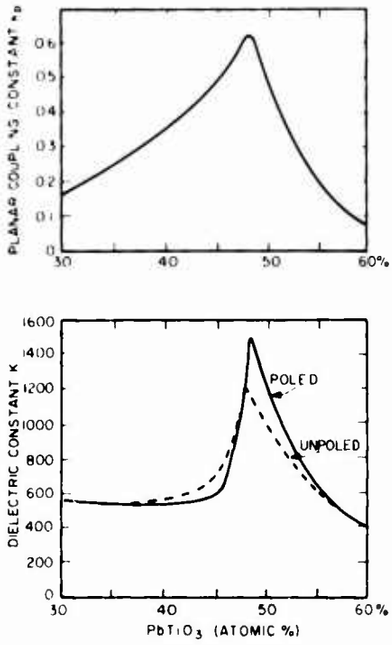

Fig. 21 - Dependence of the planar coupling constant k_p and dielectric constant K on concentration of $PbTiO_3$ in PZT

Not all compositions in the full range of PZT are equally useful for applications. Figure 21 shows that the dielectric constant K and the planar coupling factor k_p are largest in the region of the morphotropic boundary. These data are from Weston, Webster, and McNamara (13). Qualitatively similar, though less precise, results were published earlier by Jaffe, Roth, and Marzullo (14). The decrease of these constants to such small values at the 60% concentration of $PbTiO_3$ is believed to be due to the effect of the increased tetragonality. At still higher concentrations, one would expect even smaller values.

The compositions of lead zirconate-titanate useful for sonar applications are chosen to be near the morphotropic phase boundary and are further modified by both major and minor additions of chemicals for the purpose of improving specific properties such as the stability, high drive properties, or dielectric constant. For example, the Clevite Corporation has introduced a series of PZT compositions under the trade names PZT-4, PZT-5, and PZT-8, each designed for different applications. The effect of these additives on aging will be discussed below.

Aging of the Parameters

The aging of the dielectric constant of PZT is analogous to that of the dielectric constant of $BaTiO_3$ as described earlier. Figure 22 shows the aging of the permittivity (a quantity proportional to the dielectric constant) of PZT-4, as measured by Germano (15). The behavior is represented by the line labeled "normal average aging." Figures 23 and 24 show normal-average-aging curves for the planar coupling coefficient and the frequency constant, respectively. The last quantity is the product of the resonant frequency and the disk radius and is therefore proportional to the velocity of sound.

Figures 22 through 25 also show the results of 1-hour heat treatments of various samples at 175° C or at 150° C 12 days after poling. In some instances, the quantity recovers all or most of its initial value. Of importance to transducer applications is the fact that

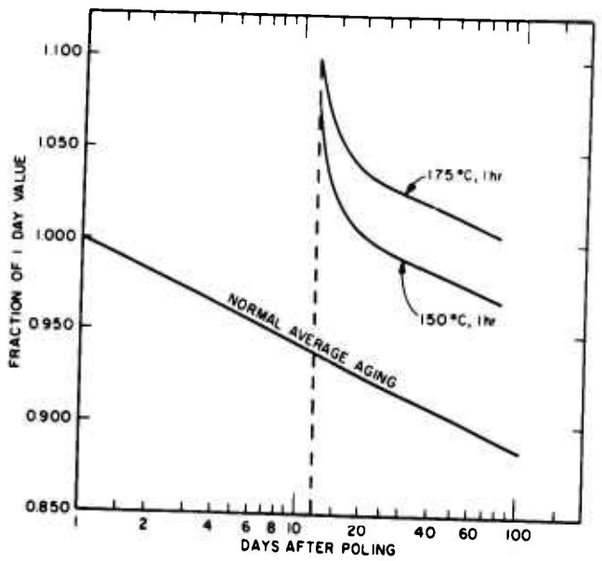

Fig. 22 - Effect of exposure to elevated temperatures on aging of the permittivity of PZT-4

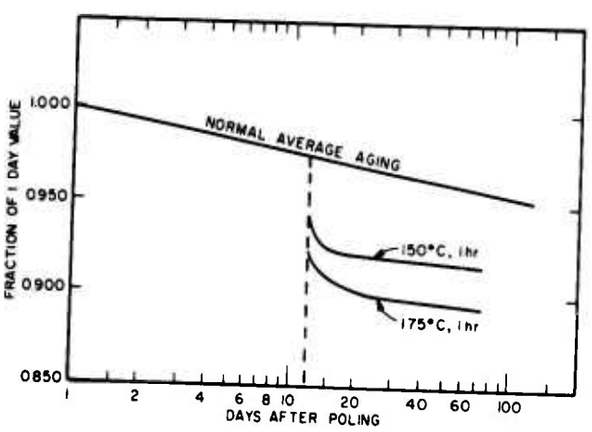

Fig. 23 - Effect of exposure to elevated temperatures on aging of the coupling factor of PZT-4

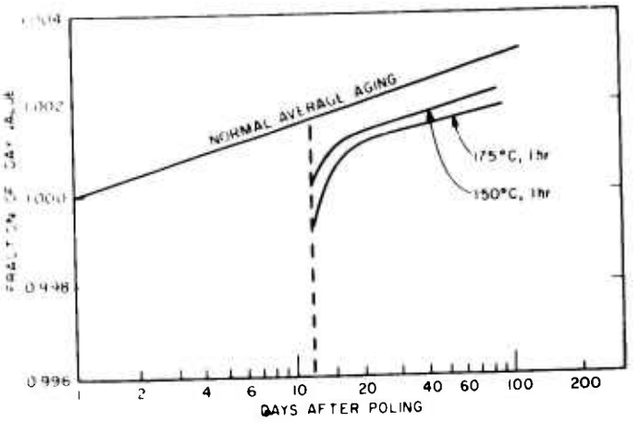

Fig. 24 - Effect of exposure to elevated temperatures on aging of the frequency constant of PZT-4

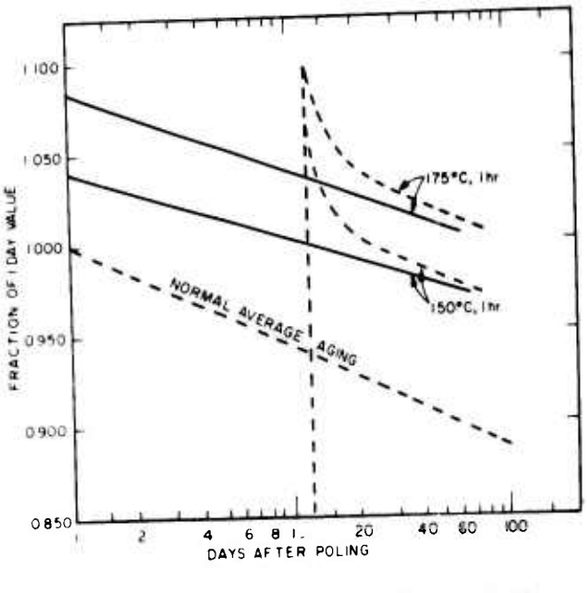

Fig. 25 - The broken lines and curves are identical with those of Fig. 22 on the aging of the permittivity of PZT-4. The solid lines are replots of the curves with the time origin shifted to the first day of heat treatment (new time equals old time minus 12 days).

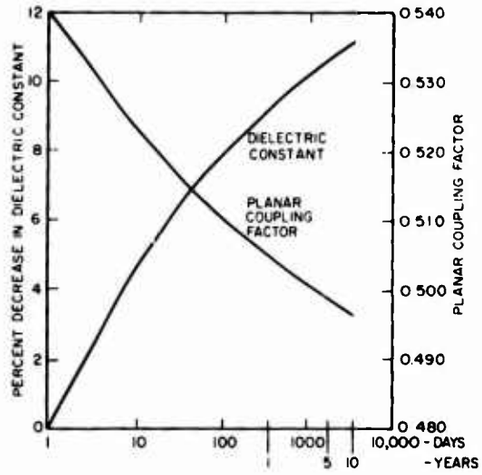

Fig. 26 - Long-term aging of PZT-4, showing departure from a strict logarithmic time dependence

heat treatment degrades the coupling constant (Fig. 23). In all cases, according to these graphs, the quantities start aging again, eventually reaching the straight-line logarithmic time dependence. The rapid change in the quantity during the first few days following the heat treatment is mainly an artifact arising from the manner of plotting. What is plotted is essentially $Q = Q(1)[1 - \beta \log (12 + t)]$. Berlincourt (16) has pointed out that if the origin of time for these plots is shifted so that the time scale begins at the time of the heat treatment, an ordinary straight line results. This is illustrated in Fig. 23 by the solid curves. These are replots of the 175°C and 150°C data of Fig. 22 on the aging of the permittivity. The broken curves in Fig. 25 are a copy of the curves of Fig. 22. An analytical discussion of this phenomenon is given in Appendix A.

It is interesting to compare these results with the "rule" for the heat treatment of $BaTiO_3$. There, the high-temperature treatment was carried out above the transition temperature and for only a few minutes. Here the treatment takes place below the transition temperature. Both results have in common the fact that the measured quantity is changed by heat treatment and ages from this new value at essentially the same rate that it did before the treatment.

One can hardly expect the relation $Q = Q(1)\ (1 - \beta \log t)$ to continue indefinitely, for a time would eventually be reached at which Q would change sign. An indication that there is a departure from this empirical law is shown in Fig. 26, taken from Berlincourt (17). This gives the aging of the coupling coefficient and dielectric constant over a period of nearly 10 years.

Effect of Chemical Additives on the Aging of PZT

The aging of the properties of PZT compositions near the morphotropic phase boundary can be appreciably affected by the addition of a percent or so of certain types of chemical additives. The kinds of additives which have been used to modify PZT have been classified by Jaffe (18) into four categories, according to their effect on its semiconductor properties. These categories are: donor, acceptor, isovalent, and thermally variable impurities. Of these, the donor and thermally variable types have a marked effect on aging. Before considering the effect of each of these kinds of impurities on aging, we shall discuss the semiconductor character of unadulterated PZT.

The p-Type Character of Ordinary PZT — The p-type character of plain (undoped) PZT ceramic sintered in air was demonstrated by Gerson and Jaffe (19). Their experimental work, in which they sought to establish the mechanism responsible for this property, follows the work of Rudolph (20) on simple oxide semiconductors. First, therefore, we shall give a sketch of some of Rudolph's findings.

The oxides studied by Rudolph have simpler structures than that of PZT and as a consequence the explanation of their semiconducting properties (as observed by Rudolph) is fairly straightforward. We shall describe some of Rudolph's results. He found, for example, that BaO and SrO have a positive Seebeck coefficient, and are therefore p-type, when held at about 1100°K in an atmosphere of oxygen. The O_2 pressure at this temperature was varied from 10^{-2} torr to 10^{3} torr, the conductivity of the samples increasing with increasing pressure. His explanation was that the increase in conductivity is due to an increase in cation (Ba or Sr) vacancies with increasing O_2 pressure, these vacancies acting as acceptor centers. As another example from Rudolph's work, we select the behavior of CaO. It is n-type at 1100°K and 10^{-2} torr O_2 pressure, decreasing in conductivity with increasing O_2 pressure to about 10 torr. Here, it reaches a minimum in its conductivity, changes to p-type, and exhibits an increasing conductivity with further increase in O_2 pressure. Again, the explanation is that increasing O_2 pressure causes a corresponding increase in Ca vacancies which compensate the n-type conduction at low O_2 pressures and overcompensate at pressures in excess of 10 torr, thus rendering the material a p-type semiconductor. Rudolph found also that doping his p-type samples with ions of higher valence than that of the cation was equivalent to adding compensating electrons to the samples, with a resulting reduction in conductivity. Doping with ions of lower valences caused the number of hole carriers to increase and the conductivity was thereby enhanced.

Gerson and Jaffe (19) ran similar measurements on doped and undoped PZT and obtained analogous results. They conjectured therefore that the p-type character of PZT sintered in air was due to Pb vacancies and that doping with donor or acceptor impurities diminishes or enhances, respectively, the hole conductivity of PZT.

Effects of Donors on Aging — Extensive measurements of the properties of PZT of composition $Pb(Zr_{0.54}Ti_{0.46})O_3$ doped with trivalent and pentavalent impurities were made by Kulcsar (21). The additions were trivalent La and Nd (in the form of La_2O_3 and Nd_2O_3) replacing bivalent Pb and pentavalent Nb and Ta (in the form Nb_2O_5) replacing tetravalent Zr and Ti. This kind of doping increased the resistivity of the PZT by a factor of 1000. Furthermore, Kulcsar observed that the grain size was reduced to about 1/2 to 1/4 the linear dimensions of the undoped material.

The effect on aging is to lower the aging rate by a factor of 5 to 10. Figure 27 shows the aging of three of the parameters of unadulterated PZT. These parameters are the dielectric constant K, the planar coupling constant k_p, and the frequency constant f_p. Figure 28 shows the reduction in the aging of these parameters when trivalent Nd or La is added. Figure 29 shows the reduction in the aging of the same parameters as a result of doping with pentavalent Nb or Ta.

Gerson (22) explains these findings in the following way. For ordinary PZT, cooling from the transition temperature (ca. 360°C) to room temperature results in large internal stresses in the ferroelectric ceramic. Aging is simply the gradual relieving of these stresses by domain wall motions. The addition of donor impurities to PZT increases the number of vacancies in such a manner that the valency balance at the Pb position is maintained. These vacancies greatly enhance the domain wall mobility. Consequently, most of the internal stresses which arise on cooling the samples are immediately relieved by domain wall motion. The observed low aging is then due to the gradual reduction of the remaining stresses.

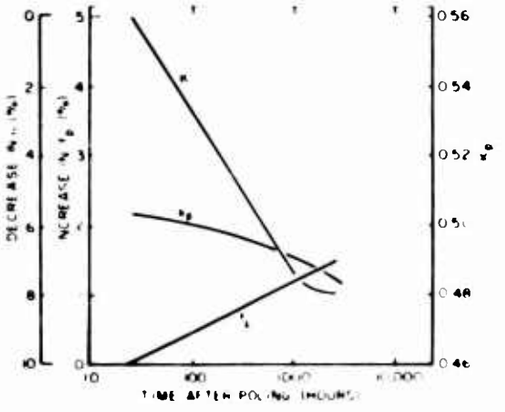

Fig. 27 - Aging of $Pb(Zr_{0.54}Ti_{0.46})O_3$ with no additions (Ref. 21)

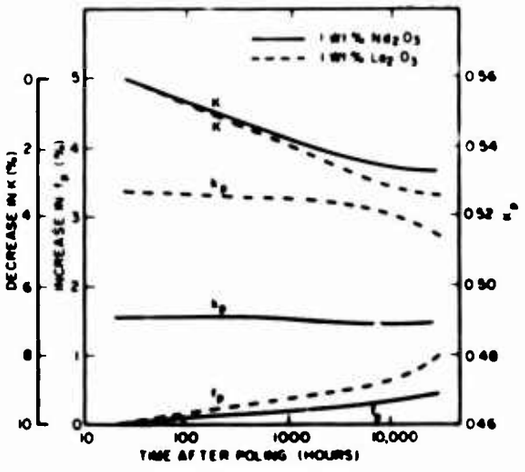

Fig. 28 - Aging of $Pb(Zr_{0.54}Ti_{0.46})O_3$ with additions of La_2O_3 and Nd_2O_3

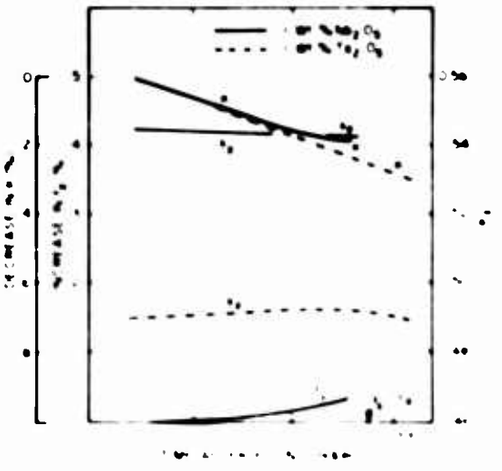

Fig. 29 - Aging of $Pb(Zr_{0.54}Ti_{0.46})O_3$ with additions of Nb_2O_5 and Ta_2O_5

The Clevite Corporation PZT-5 family of materials consists of these donor-doped ferroelectric ceramics (18).

Effect of Acceptors on Aging — The Clevite Corporation PZT-8 ferroelectric ceramics consist of PZT doped with acceptor ions (18). These ions are of a lower valence than those which they replace in the parent material. The ion K^+ replaces Pb^{2+}, while Sc^{3+}, Fe^{3+}, and Mg^{2+} replace either Zr^{4+} or Ti^{4+}. These impurities cause an oxygen deficiency, and it is believed that the resulting oxygen vacancies pin the domain walls, thereby reducing their mobility. As a consequence, the aging rate remains about the same value as that of the undoped material.

Effect of Isovalent Additions on Aging — PZT doped with isovalent additives form the PZT-4 class of Clevite materials (18). The additives are ions of the same valence and of about the same size as those they replace in the parent material.

Jaffe (18) distinguishes two classes of isovalent additives: simple and complex. Examples of simple additives are Ca, Ba, Sr, Sn, Hf, and Cd. Examples of complex isovalent additives are $BiFeO_3$, $(Mg_{0.5}W_{0.5})^{4+}$, and $(Na_{0.5}La_{0.5})^{2+}$. The simple additives do not improve aging. Jaffe states that the effect of the complex additives on aging is not yet clear (in 1969, the date of Ref. 18).

Effect of Thermally Variable Ions on Aging — Thermally variable ions are ions whose valence is temperature dependent (18). To this class of additives belong Cr, U, and perhaps Mn. According to Jaffe (18), such additives lower the aging rate.

Combinations of ions such as these, together with acceptors, provide the possibility of producing sonar transducer materials having both good high-drive and low aging properties. The difficulty hitherto has been that these qualities were mutually exclusive: good high-drive characteristics are a result of pinned domain walls and low aging is a result of domain wall mobility. Examples of good high-drive materials are Clevite's PZT-4 and PZT-8. The former is PZT with 6 atom percent of the isovalent ion Sr^{2+} present, and the latter is PZT doped with isovalent ions and acceptors. Both PZT-4 and PZT-8 suffer from rather high aging rates (several percent per decade for the pertinent parameters). It occurred to the research staff at the Clevite Corporation (23) that a combination of thermally variable additives with donors and acceptors might yield a material whose high-drive properties compete with those of PZT-4 yet whose aging rate is low. Various combinations of the dopants Cr, Fe, U, and Nb were tried. The result was the combination

$$Pb_{0.94}Sr_{0.06}(Zr_{0.525}Ti_{0.475})_{0.98}Cr_{0.015}Fe_{0.005}O_3,$$

with about one-tenth the aging rate of PZT-4 and almost as good high-drive properties up to stresses of 10 kpsi. In the range 10 to 20 kpsi, the properties unfortunately degrade. In the course of these experiments, it was found that the same material with 6 atom percent of Ca replacing the 6 atom percent Sr held considerable promise and should be investigated (23).

RESEARCH SUGGESTIONS

Single Crystals

Single crystals of PZT, near the morphotropic phase boundary (doped and undoped) should be grown and their properties and domain structure studied. Without a knowledge of these single-crystal properties, an analysis of the behavior of the more complicated ceramic form of these materials remains at too conjectural a level. This has a bearing on the other research suggestions made here.

90°-Domain Formation During Aging

Studies of the 90°-domain formation, such as was done by Bradt and Ansell for $BaTiO_3$, should be undertaken for the various PZT compounds: those containing donor, acceptor, or thermally variable ions. For example, donor additives lower the aging rate by a factor of 5 to 10. Is this because much of the aging has occurred during the first few seconds or minutes? If so, does the 90°-domain structure of such a substance at the earliest time of observation resemble that of ordinary PZT when the latter is at an advanced age? Or is the opposite true?

Theory of Aging

The theory of aging outlined in this report does not really do justice to the 90°-domain formation phenomenon. For example, the nature of the traps remains unspecified, internal stresses are not mentioned, and no provision is made for the formation of new walls. It is evident that an improved theory is needed. Ikegami and Ueda (7) have already made a start in this direction with their treatment of the motion of a 90°-domain wall along a whisker under stress.

Thermally Variable Ions

The behavior of thermally variable ions (such as chromium) is not yet understood. One needs a better understanding of the basic physics of thermally variable valence as well as more information concerning the structure and properties of PZT containing such dopants.

Heat Treatment Effects

The Germano type of heat treatment partially restores the dielectric constant K to its initial value but degrades the coupling constant k. What is the explanation of this?

REFERENCES

1. Marks, B.H., "Ceramic Dielectric Materials," Electronics 21:116 (1948)

2. McQuarrie, M.C., and Buessem, W.R., "The Aging Effect in Barium Titanate," Am. Ceram. Soc. Bull. 34:402 (1955)

3. Mason, W.P., "Aging of the Properties of Barium Titanate and Related Ferroelectric Ceramics," J. Acoust. Soc. Amer. 27:73 (1955)

4. Pleasner, K.W., "Aging of the Dielectric Properties of Barium Titanate Ceramics," Proc. Phys. Soc. (London) 69B:1261 (1956)

5. Smith, C.L., "A Theory of Transient Creep in Metals," Proc. Phys. Soc. (London) 61:201 (1948)

6. Street, R., and Woolley, J.C., "A Study of Magnetic Viscosity," Proc. Phys. Soc. (London) 62A:562 (1949)

7. Ikegami, S., and Ueda, I., "Mechanism of Aging in Polycrystalline $BaTiO_3$," J. Phys. Soc. Japan 22:725 (1967)

8. Bradt, R.C., and Ansell, G.S., "Aging in Tetragonal Ferroelectric Barium Titanate," J. Am. Ceram. Soc. 52:192 (1969)

9. Bradt, R.C., "The Aging Phenomenon in Barium Titanate," Ph.D. Thesis (1967), Rensselaer Polytechnic Institute, Microfilm-xerograph by University Microfilms, Ann Arbor, Mich. (1969)

10. Stankowski, J., "Aging in $BaTiO_3$ Ceramics," Bull. Soc. Amis. Sci. Lettres Poznan Ser. B16:27-59 (1960-61) (published 1962)

11. Sawaguchi, E., "Ferroelectricity versus Antiferroelectricity in the Solid Solutions of $PbZrO_3$ and $PbTiO_3$," J. Phys. Soc. Japan 8:615 (1953)

12. Shirane, G., Suzuki, K., and Takeda, A., "Phase Transitions in Solid Solutions of $PbZrO_3$ and $PbTiO_3$, (II) X-Ray Study," J. Phys. Soc. Japan 7:12-18 (1952)

13. Weston, T.B., Webster, A.H., and McNamara, V.M., "Variations in Properties with Composition in Lead Zirconate-Titanate Ceramics," J. Can. Ceram. Soc. 36:15 (1967)

14. Jaffe, B., Roth, R.S., and Marzullo, S., "Piezoelectric Properties of Lead Zirconate-Lead Titanate Solid-Solution Ceramics," J. Appl. Phys. 25:809 (1954)

15. Germano, C.P., "Effect of Exposure to Elevated Temperatures on Aging of Frequency Constant, Coupling Constant, and Dielectric Permittivity of PZT-4," Engineering Memorandum PD-65-1, Piezoelectric Division, Clevite Corporation, Bedford, Ohio, 1965

16. Berlincourt, D., Letter Memorandum at the Clevite Corporation (see Ref. 6), dated Mar. 13, 1966, commenting on Germano's data

17. Berlincourt, D., "Long-Term Aging of PZT-4," Engineering Memorandum 64-11, Clevite Corporation (see Ref. 15), 1964

18. Jaffe, B., "Effects of Compositional Variations in $Pb(Ti,Zr)O_3$ Solid Solutions," Seminar on Piezoelectric Ceramics and Devices held at the Statler-Hilton Hotel, Cleveland, Ohio, Oct. 9-10, 1969

19. Gerson, R., and Jaffe, H., "Electrical Conductivity in Lead Titanate Zirconate Ceramics," J. Phys. Chem. Solids 24:979 (1963)

20. Rudolph, J., "Über den Leitungsmechanismus oxydischer Halbleiter bei hohen Temperaturen," Z. Naturf. 14a:727 (1959)

21. Kulcsar, F., "Electromechanical Properties of Lead Titanate Zirconate Modified with Certain Three- or Five-valent Additions," J. Am. Ceram. Soc. 42 (No. 7):343-9 (1959)

22. Gerson, R., "Variation in Ferroelectric Characteristics of Lead Zirconate Titanate Ceramics Due to Minor Chemical Modifications," J. Appl. Phys. 31 (No. 1):188-194 (1960)

23. Jaffe, B., and Krueger, H.H.A., "Research on Higher Power Transducer Ceramics, Development of Low Aging Compositions for Sonar Applications," Report dated Nov. 10, 1967 on Contract Nonr-3958(00), Department of the Navy, Office of Naval Research

Appendix A

SEMILOG PLOTTING

In this appendix, it is shown that a transfer of the origin of the abscissa in a semilog plot results in a distortion of a straight line to a curve.

Let us assume that a quantity $Q(t)$ is found to obey the empirical relation

$$Q(t) = Q(1)\ (1 - \beta \log t),\ t \geq 1. \tag{1a}$$

At the time $t = 1$, we have $Q(t) = Q(1)$. Let us introduce the abbreviated notation of $q = Q(t)/Q(1)$. Then Eq. (1a) becomes

$$q = 1 - \beta \log t,\ t \geq 1. \tag{2a}$$

A plot of q versus t on semilog paper will yield a straight line of slope

$$dq/d(\log t) = -\beta.$$

Suppose, now that the origin of the time is shifted to $t = t_0$. Then Eq. (2a) can be written as

$$q = 1 - \beta \log(t + t_0 - t_0)$$

or

$$q = 1 - \beta \log (\tau - t_0),\ \tau \geq 1 + t_0. \tag{3a}$$

Here, we have substituted τ for $t + t_0$, a new time.

The relation in the form of Eq. (3a) is exactly the same as when it was in the form of Eq. (2a); that is, the physical law was not changed. However, when q versus τ is plotted instead of q versus t, the resulting plot is not a straight line. Yet such a plot is likely to be made when a table of numerical values of Q versus τ is given, though it is not likely to be made from Eq. (3a) since its derivation is known. The effect of this time shift on the shape of the new curve is easily seen by comparing the slope $dq/d\ (\log \tau)$ with the slope $dq/d\ (\log t) = -\beta$. To obtain the slope $dq/d\ (\log \tau)$, set $x = \log \tau$ (or $\tau = e^x$) into Eq. (2a) and obtain the required derivative by the series of operations:

$$q = 1 - \beta \log (e^x - t_0)$$

and

$$\frac{dq}{dx} = -\beta \frac{e^x}{e^x - t_0} = -\beta \frac{\tau}{\tau - t_0}.$$

Therefore, we have for the ratio of the slopes:

$$\frac{dq}{d(\log \tau)} \Big/ \frac{dq}{d(\log t)} = \frac{\tau}{\tau - t_0}. \tag{4a}$$

At $\tau = t_0$ (not allowed, however, since $\tau \geq 1 + t_0$), the ratio is infinite. At $\tau = 1 + t_0$, the ratio is $1 + t_0$. As τ approaches infinity ($\tau >> t_0$), the ratio approaches unity and the new curve approaches the straight line given in Eq. (2a).

Security Classification

DOCUMENT CONTROL DATA - R & D

(Security classification of title, body of abstract and indexing annotation must be entered when the overall report is classified)

1. ORIGINATING ACTIVITY (Corporate author)	2a. REPORT SECURITY CLASSIFICATION
Naval Research Laboratory Washington, D.C. 20390	Unclassified
	2b. GROUP

3. REPORT TITLE

AGING OF BARIUM TITANATE AND LEAD ZIRCONATE-TITANATE FERROELECTRIC CERAMICS

4. DESCRIPTIVE NOTES (Type of report and inclusive dates)

An Interim report reviewing the present state of knowledge of the aging process.

5. AUTHOR(S) (First name, middle initial, last name)

Jules deLaunay and Paul L. Smith

6. REPORT DATE	7a. TOTAL NO. OF PAGES	7b. NO. OF REFS
October 15, 1970	30	23

8a. CONTRACT OR GRANT NO.	9a. ORIGINATOR'S REPORT NUMBER(S)
NRL Problem P03-03 b. PROJECT NO. SF 11-121-303/14082 c. d.	NRL Report 7172
	9b. OTHER REPORT NO(S) (Any other numbers that may be assigned this report)

10. DISTRIBUTION STATEMENT

This document has been approved for public release and sale; its distribution is unlimited.

11. SUPPLEMENTARY NOTES	12. SPONSORING MILITARY ACTIVITY
	Department of the Navy (Naval Ship Systems Command), Washington, D.C. 20360

13. ABSTRACT

The report reviews the present knowledge of the aging process in barium titanate and lead zirconate-titanate ferroelectric ceramics. By "aging" is meant the passive change in the mechanical and electrical properties of a ferroelectric with time. Experimental data show that these constants vary linearly with the logarithm of time. The Smith, Street and Woolley, and Plessner theories for this logarithmic dependence are revised to remove some of the obscurity in the usual derivation. The experimental evidence of Ikegami and Ueda and of Bradt and Ansell, which is described in some detail, supports the hypothesis that aging is associated with the relief of internal stress through the formation of 90°-domains.

The properties of lead zirconate-titanate can be changed to some extent by chemical additives. Such additions may also change the aging rate. In particular, it has been found that trivalent and pentavalent ions substituted for bivalent lead decrease the rate by a factor of 5 to 10. On the other hand, additives which cause an oxygen deficiency (e.g., Fe) have little effect on the aging rate. A class of chemicals (e.g., Cr) called "thermally variable ions" by Jaffe, because of the apparent temperature dependence of their valence, holds promise for lowering the aging rate without adversely affecting the high-drive sonar transducer characteristics of the material.

Suggestions are made for further research.

DD FORM 1 NOV 65 1473 (PAGE 1)

S/N 0101-807-6801

Security Classification

14 KEY WORDS	LINK A		LINK B		LINK C	
	ROLE	WT	ROLE	WT	ROLE	WT
Ferroelectrics						
Ceramics						
Aging						
Barium titanate						
Lead zirconate-titanate						